Journal of Applied Polymer Science

Flurbiprofen axetil loaded coaxial electrospun poly(vinyl pyrrolidone)–nanopoly(lactic-*co*-glycolic acid) core–shell composite nanofibers: Preparation, characterization, and anti-adhesion activity

Tonghe Zhu,[1,2] Sihao Chen,[2,3] Wenyao Li,[4] Jianzhong Lou,[2,3,5] Jihu Wang[2,3]

[1]School of Fashion Design, Shanghai University of Engineering Science, Shanghai 201620, People's Republic of China
[2]Multidisciplinary Center for Advanced Materials, Shanghai University of Engineering Science, Shanghai 201620, People's Republic of China
[3]College of Chemistry and Chemical Engineering, Shanghai University of Engineering Science, Shanghai 201620, People's Republic of China
[4]School of Materials Engineering, Shanghai University of Engineering Science, Shanghai 201620, People's Republic of China
[5]Department of Chemical Engineering and Biomedical Engineering, North Carolina A&T State University, 1601 East Market Street, Greensboro North Carolina 27411
Correspondence to: S. Chen (E-mail: chensh@sues.edu.cn) and W. Li (E-mail: liwenyao314@gmail.com)

ABSTRACT: Flurbiprofen axetil (FA)-loaded coaxial electrospun poly(vinyl pyrrolidone) (PVP)–nanopoly(lactic-*co*-glycolic acid) core–shell composite nanofibers were successfully fabricated by a facile coaxial electrospinning, and an electrospun drug-loaded system was formed for anti-adhesion applications. The FA, which is a kind of lipid microsphere nonsteroidal anti-inflammatory drug, was shown to be successfully adsorbed in the PVP, and the formed poly(lactic-*co*-glycolic acid) (PLGA)/PVP/FA composite nanofibers exhibited a uniform and smooth morphology. The cell viability assay and cell morphology observation revealed that the formed PLGA/PVP/FA composite nanofibers were cytocompatible. Importantly, the loaded FA within the PLGA/PVP coaxial nanofibers showed a sustained-release profile and anti-adhesion activity to inhibit the growth of the IEC-6 and NIH3T3 model cells. With the significantly reduced burst-release profile, good cytocompatibility, and anti-adhesion activity, the developed PLGA/PVP/FA composite nanofibers were proposed to be a promising material in the fields of tissue engineering and pharmaceutical science. © 2015 Wiley Periodicals, Inc. J. Appl. Polym. Sci. **2015**, *132*, 41982.

KEYWORDS: biomaterials; electrospinning; fibers

Received 24 July 2014; accepted 14 January 2015
DOI: 10.1002/app.41982

INTRODUCTION

Electrospinning is a popular nanotechnology for producing nanofibers because of its ease of implementation and cost effectiveness; it also results in unique properties of and versatile applications for the resulting nanofibers. The features of electrospun nanofibers, with their high specific surface area, high porosity, and three-dimensional reticulate structure, mimic the natural extracellular matrix; this affords them with a wide range of biomedical applications, including in tissue engineering, wound dressing, biosensors, and drug delivery.[1–4] In particular, for drug-delivery applications, conventional, emulsion, and coaxial electrospinning techniques have been used to fabricate nanofibers for drug encapsulation and release.[5,6] In recent decades, the electrospinning process has developed from its use of a single fluid to that of two fluids (coaxial and side-by-side electrospinning) and even multiple fluids (multiple coaxial electrospinning).[5,7,8] These techniques allow for the creation of new types of sophisticated nanofibers with well-defined microstructures, novel morphologies, and new functions. Furthermore, they widen the capability of the simple one-step process to generate new advanced nanofiber materials. One of them is the coaxial electrospinning process, in which a concentric spinneret can accommodate two different fluids for the fabrication of core–shell structures;[9–12] this is regarded as one of the most significant breakthroughs in this field, and it has drawn increasing attention.

A conventional single-fluid electrospinning method allows the direct integration of drug molecules within nanofibers by the

© 2015 Wiley Periodicals, Inc.

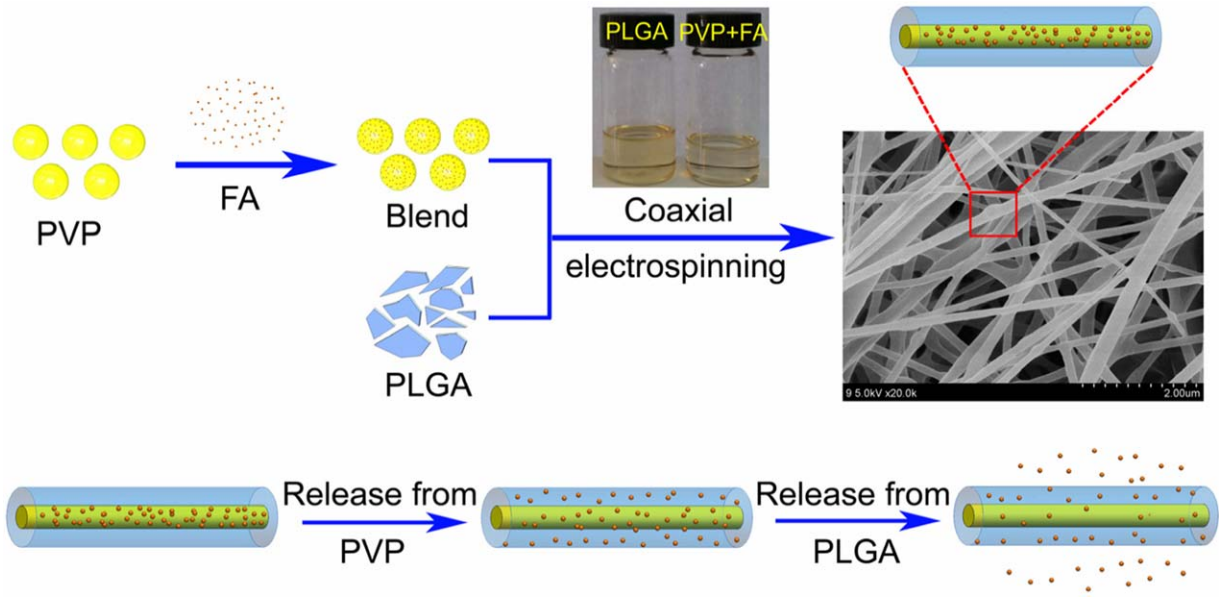

Figure 1. Schematic illustration of the encapsulation and release pathways of FA within core–shell structure PLGA/PVP/FA nanofibers. [Color figure can be viewed in the online issue, which is available at wileyonlinelibrary.com.]

simple electrospinning of the drug/polymer mixture solution or postadsorption of drugs onto/within the nanofibers.[13,14] However, a burst release often happens, which is not desirable in most cases. The techniques of coaxial electrospinning used for drug-delivery applications are able to alleviate the burst release of the encapsulated drug to some extent.[5,12,15–17] In this method, the drugs are able to be incorporated into the core region of the nanofibers to form a core–shell structure, in which the outer polymer shell can act as an additional barrier to control the drug-release profile. The modified coaxial process opens a new route for the generation of nanofibers from polymer solutions by the partial replacement of the traditional interface between polymer jets and the atmosphere via the interface between electrospinnable core polymer jets and shell solvents.[18–22]

Poly(lactic-*co*-glycolic acid) (PLGA) fibers have been considered as an ideal organic drug carrier because of their high surface-area-to-volume ratio, high surface activity, good biocompatibility, and strong ability to absorb a variety of chemical species.[23–25] However, the weak interaction between the drug molecules and the nanofibers preparation by electrospinning (*n*-PLGA) particles often leads to an initial burst release of the drugs from the formed PLGA/drug nanocomplex. Therefore, it is quite reasonable to design a hybrid nano-PLGA-incorporated polymer nanofiber system, where both the polymer nanofibers and PLGA are containers and barriers of drug molecules and afford the drug with a sustained-release profile.[24,26–29] Likewise, the presence of PLGA within the polymer nanofibers is also expected to share a portion of load applied on the nanofibrous mats; this improves the mechanical durability of the fiber system.[30–35]

In this study, we fabricated poly(vinyl pyrrolidone) (PVP)-doped PLGA nanofibers via electrospinning for drug encapsulation and release. A model drug, flurbiprofen axetil (FA) was first loaded in the PVP via physical blending. Then, we used coaxial electrostatic spinning of the FA-loaded PVP with PLGA solution to form PLGA/PVP/FA composite nanofibers (Figure 1). The incorporation of the drug-loaded PLGA/PVP nanofibers not only improved the adhesion prevention activity of the nanofibers significantly, but it also appreciably reduced the initial burst release of the drug. This is important for biomedical applications requiring drugs to maintain long-term analgesic efficacy.

EXPERIMENTAL

Materials

PLGA (weight-average molecular weight = 100,000 g/mol) with a lactic acid/glycolic acid ratio of 75 : 25 and FA (purity>99%) were purchased from Jinan Daigang Biotechnology Co., Ltd. (Jinan, China) and Shanghai Xinya Pharmaceutical Co., Ltd. (Shanghai, China), respectively. PVP (K30) was obtained from Shanghai Zhanyun Chemical Co., Ltd. (Shanghai, China). Luria–Bertani medium was acquired from Sangon Biotech Co., Ltd. (Shanghai, China). Dichloromethane, absolute ethanol (EtOH), and *N*,*N*-dimethylformamide (DMF) were obtained from Shanghai Lingfeng Chemical Reagent Co., Ltd. (Shanghai, China). IEC-6 cell and NIH3T3 cell were obtained from the Institute of Biochemistry and Cell Biology (The Chinese Academy of Sciences, Shanghai, China). Dulbecco's Modified Eagle's Medium, fetal bovine serum, glutaraldehyde, 3-(4,5)-dimethylthiahiazo (-z-yl)-3,5-di-phenytetrazoliumromide (MTT), Cell counting kit-8 is WST-8 [2-(2-methoxy-4-nitrophenyl)-3-(4-nitrophenyl)-5-(2,4-disulfophenyl)-2H-tetrazolium, monosodium salt] (CCK-8), acridine orange, ethidium bromide, and a live/dead cell staining kit were purchased from Shanghai Limin Industrial Co., Ltd. (Shanghai, China). A commercial membrane (polylactide (PLA), anti-adhesion membrane) was purchased from Chengdu Branch Dikang Biomedical Materials Co., Ltd. (Chengdu, China). All of the chemicals were used as received. The water used in all of the experiments was purified with a Milli-Q Plus

185 water purification system (Millipore, Bedford, MA) with a resistivity of higher than 18 MΩ cm.

Fabrication of Composite Nanofibers with Core–shell Structure

PLGA (10 wt %) was dissolved in a mixture of dichloromethane and DMF with a volume ratio of 3 : 1 as shell layer solution. A mixture of EtOH and DMF (volume ratio 2 : 1) used as the solvent for dissolving PVP and FA at a concentration of 6 wt % as core layer solution. The mixture solution of shell layer and core layer was stirred for more than 8 h and ultrasound about 5 min before use.

The coaxial spinneret consisted of two concentrically arranged capillaries. The inner capillary had inner and outer diameters of 0.35 and 0.65 mm, respectively, whereas the outer capillary had inner and outer diameters of 1.05 and 1.20 mm, respectively. Volumes of 10 mL of PLGA solution and 10 mL of PVP with FA solutions were contained in two individual syringes and connected to the coaxial spinneret. The flow rates in the capillaries were controlled by two separate pumps. Both capillaries were connected to the same high-voltage power supply. The coaxial electrospun nanofibers were collected on an aluminum foil placed above the flat, grounded metal plate. The applied voltage and the distance between the tip of the spinneret and the collector were maintained at 20 kV and 14 cm, respectively. The shell flow rate was set to 1.0 mL/h, whereas the core flow rate was varied from 0.1 to 0.4 mL/h. All of the electrospinning processes were carried out at around 25°C and 50% relative humidity.

Material Characterization

The as-prepared products were characterized with Fourier transform infrared (FTIR) spectrometry (Nicolet Avatar 380), video water contact angle (WCA) measurement (Samsung FA-CED camera), field emission scanning electron microscopy (SEM; HITACHI S-4800), and transmission electron field electron microscopy (TEM; JEOL JEM-2100).

In Vitro Drug Release

All of the samples for the release experiments were incubated in a vapor-bathing, constant-temperature vibrator at 37°C with a vibrating speed of 100 rpm. The experiment was done in triplicate. At scheduled time intervals (2, 6, 10, 18, 26, 34, 48, 60, 84, 108, 132, 156, 180, and 204 h), 3 mL of sample was taken, and fresh phosphate-buffered saline (PBS) medium with an identical volume was added to maintain vapor-bathing, constant-temperature vibrator conditions. The mass of FA released at time t, mass of released FA at time t (M_t), and total drug amount (M_{tot}) were determined with a Lambda 25 ultraviolet–visible spectrophotometer (PerkinElmer) at 254 nm in PBS. The drug loading was determined with eq. (1). The percentage of released drug was calculated with eq. (2). Calculations of the amount of released drug took into account replacement with fresh medium at each sampling point. Controls (fibers without drug) were also tested, and their contribution to the absorbance was subtracted:

$$\text{Loading percentage } (\%) = \frac{M_{tot}}{M_{fiber}} \times 100\% \quad (1)$$

where M_{fiber} is the mass of the fiber mat, respectively:

$$\text{Released drug } (\%) = \frac{M_t}{M_{tot}} \times 100\% \quad (2)$$

The accumulated release of FA was calculated on the basis of a standard FA absorbance concentration calibration curve at 254 nm.

The percentage of accumulated release could be calculated by the following equation:

$$\text{ARP } (\%) = \frac{C \times 30 + \sum W}{m \times R \times 1000} \times 100\% \quad (3)$$

where C is the concentration of FA (μg/mL), ΣW is the mass of FA accumulated release (μg), m is the mass of the fiber mat (mg), and R is the percentage of drug within the fiber.

Cell Culture and Cytocompatibility Evaluation

The electrospun mats of the PLGA/PVP/FA core–shell composite nanofibrous membranes were dried *in vacuo* for 24 h at 25°C before the cytocompatibility evaluation and the anti-adhesion test were carried out. The prepared PLGA/PVP/FA composite nanofibrous membrane was cut into dimensions of 60 × 60 mm^2 and weighed. The sample was then placed into a test tube with 50 mL of PBS (pH = 7.4), and the tube was vacuumed for 20 min to allow the PBS permeate into the PLGA/PVP/FA composite nanofibers pores. After that, the test tube was placed in a homothermal oscillator (37 ± 0.1°C, 50 rpm) for 8 weeks for hydrolysis. The supernatant was collected to measure the toxicity of the PLGA/PVP/FA composite nanofiber mats.

The prepared degradation liquid was made into a medium with a concentration of 1 μL/200 μL, 10% glucose medium serous was taken as the diluent, and IEC-6 and NIH3T3 cells were inoculated into the diluent with the concentration of 2×10^4 cells/mL. The cells were inoculated for 2 and 3 days, respectively. The original medium was sucked up, 1 mL of PBS medium was added, and the material was blow-washed three times. PBS was sucked up, and 2.5–3.0% glutaraldehyde was added. The medium was allowed to stand for 2.5–3 h. Glutaraldehyde was sucked up, gradient EtOH dehydration (15 min/time) was performed with 30, 50, 75, 80, 95, and 100% EtOH (twice). After critical-point drying, SEM observation was performed.

The cells (10 cells/well) in the logarithm growth period were plated in a 96-well plate. We made sure that cell number was 6000 cells/well after 2 days of incubation; the cell numbers were 4000 and 3000 cells/well after 4 and 7 days of incubation, respectively. The plated cells were allowed to adhere the wall for 6 h at 37°C and 5% CO_2. Then, the prepared PLGA/PVP/FA composite nanofibrous membrane with a similar size as the 96-well plate was placed in the medium and immersed. After 2, 4, and 7 days of incubation, the PLGA/PVP/FA composite nanofibrous membrane was taken out, a CCK-8 test was performed for the cells, and wells without nanofibrous membrane were taken as the control wells.

In Vitro Anti-Adhesion Activity Assay

Cell adhesion to the PLGA/PVP/FA composite nanofibers membrane. PLGA/PVP/FA composite nanofibrous membrane and PLA nanofibrous membrane (commercial membrane) were cut

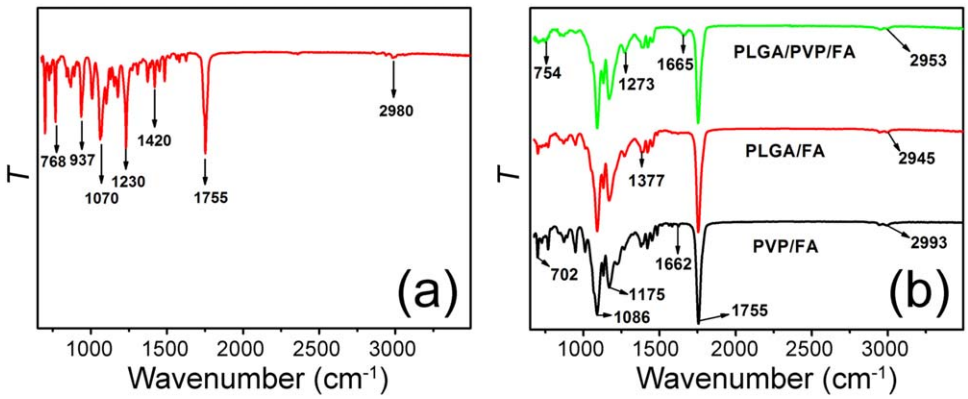

Figure 2. FTIR spectra of (a) free FA and (b) FA within PVP, FA within PLGA, and PLGA/PVP/FA. [Color figure can be viewed in the online issue, which is available at wileyonlinelibrary.com.]

into sample sizes of 50 × 20 mm^2 with thicknesses of 80 μm (sample 1), 120 μm (sample 2), 160 μm (sample 3), and 200 μm (sample 4). The samples were placed into six-well plates, six parallel holes were prepared for each nanofibrous membrane, and the covers of six well plates were opened and exposed to UV radiation for 30 min to sterilize the samples before the cells were plated. Meanwhile, the glass slides placed in six-well plates were exposed to UV radiation for 30 min. Cells (5×10^3) in 100 mL of media were plated in each well and incubated for 2, 4, and 7 days. The cell number after 2 days of inoculation was 4×10^5 cells/well. The cell number after 4 days inoculation was 4×10^4 cells/well, and the cell number after 7 days of inoculation was 4×10^3 cells/well. After inoculation, the supernatant was aspirated. Then, membranes and coverslips were transferred to new six-well plates, 1.5 mL of the MTT solution (5 mg/mL dilution by PBS solution, with culture medium diluted 10 times before use) was added to each well, and the samples were incubated for 4 h. The culture supernatant fluid in the wells was aspirated. Then, 1 mL of dimethyl sulfoxide was added to each well, and the plates were shaken for 10 min. The wavelength was selected as 490 nm, and the light absorption value of each well was detected with a microplate reader (Spectra Max M5, Molecular Devices Co., Shanghai, China. The results were recorded.

The absorbance value of the coverslip as the control or the percentage adhesion rate was calculated with the following equation:

$$\text{Adhesion ratio}(\%) = \frac{A_0 - A_i}{A_0} \times 100\% \quad (4)$$

where A_0 and A_i are the control bore absorbance value and the test absorbance value, respectively.

Cell growth on the membrane. PLGA/PVP/FA composite nanofibrous membranes and PLA nanofibrous membranes with thicknesses of 80 μm (sample 1) and 160 μm (sample 3) were cut into cubic slices with dimensions of 50 × 50 mm^2, which was similar to the size of the coverslip. The cubic slices were placed into 30-mm culture plates. The culture plates were then opened and exposed to UV radiation for 30 min. After sterilization, 4×10^5 cells were seeded into each culture plate, and the membranes were immersed in the cell culture media. Later, at 2- and 4-day time points, the supernatant was aspirated, and the membranes were transferred into new culture plates. Then, serum-free medium was added to the plate for washing. After that, acridine orange and ethidium bromide fluorochrome was added. The cells were then incubated for 40–50 min at 37°C, and subsequently, cells were imaged with a fluorescence microscope (JAOLY-670, Olympus Co., Japan). Finally, the normal cells adhered to the wall were fluorochrome-stained for control, and the cell growth conditions on the different kinds of membranes were compared.

RESULTS AND DISCUSSION

Loading of FA Blend with PVP

The successful loading of FA within PLGA/PVP was qualitatively confirmed by FTIR spectroscopy (Figure 2). In Figure 2(a), the typical absorption bands at 1070 and 1755 cm^{-1} were assigned to the C—C stretching vibrations and the carbonyl of FA, respectively. The peaks at 3000, 1755, and 1230 cm^{-1} were attributed to the absorption band of the benzene ring, the vibrations of the carbonyl group, and the stretching vibrations of the C=C group of the FA, respectively. The peak at

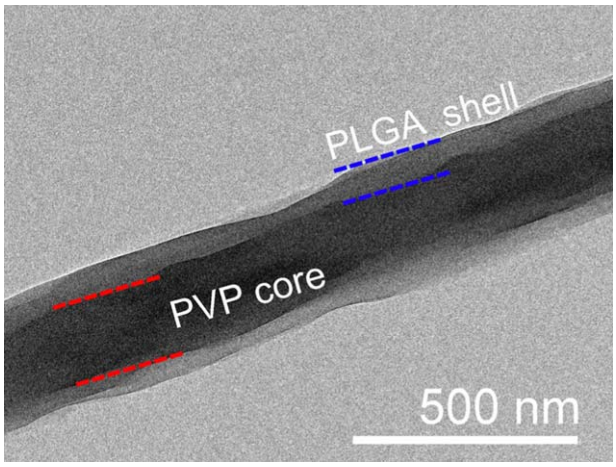

Figure 3. TEM images of the core–shell PLGA/PVP composite nanofibers. [Color figure can be viewed in the online issue, which is available at wileyonlinelibrary.com.]

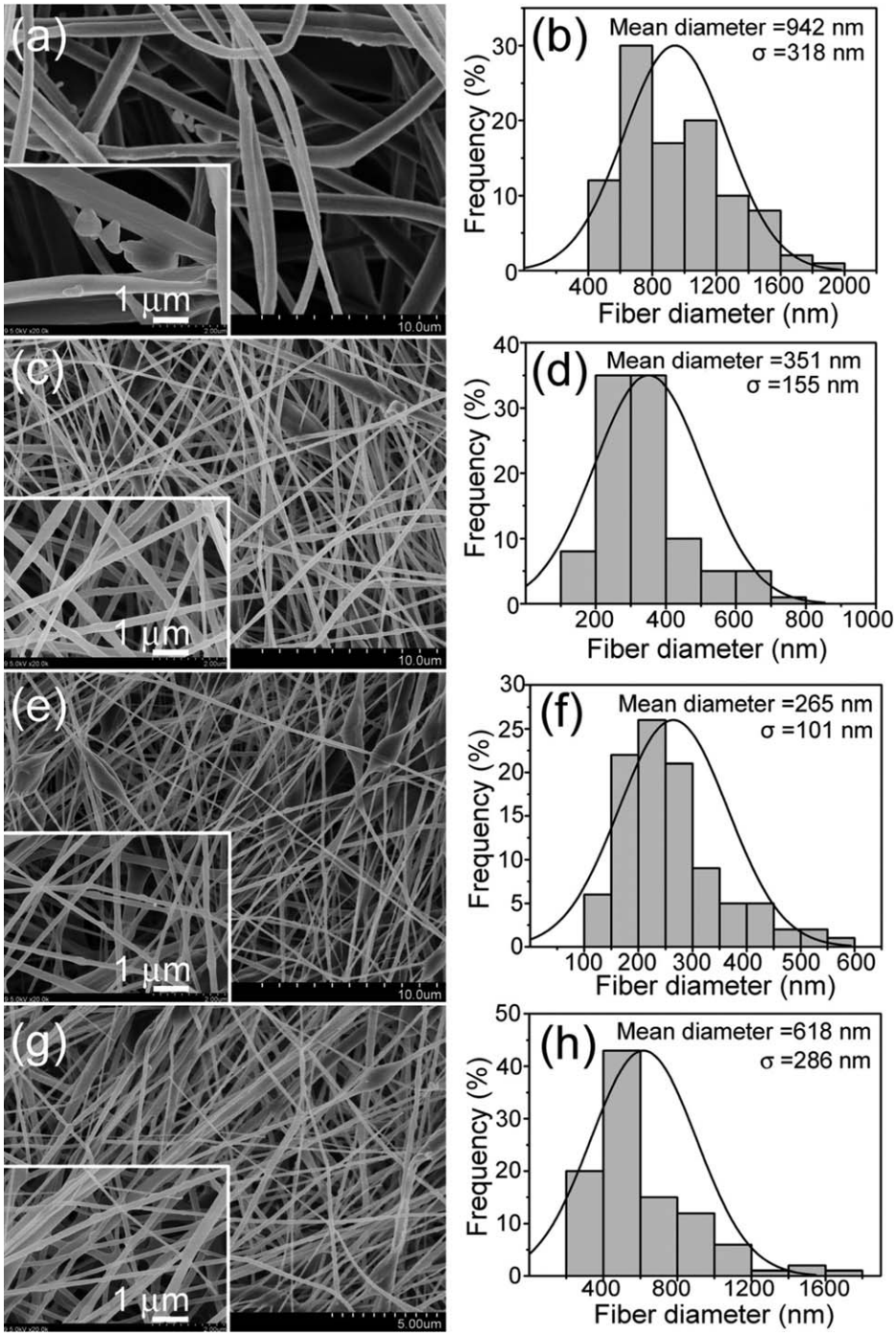

Figure 4. SEM images and diameter distribution histograms of the PLGA/FA blend fibers, PLGA/PVP/FA coaxial fibers, and PLGA/PLGA/FA coaxial fibers. σ is the standard deviation of nanofibers diameter of the sample.

1665 cm^{-1} was due to the stretching vibrations of the carbonyl group in the PVP structure. In Figure 2(b) (PLGA/PVP/FA curve), the peak at 1753 cm^{-1} was assigned to the absorption peak of the carbonyl, and the band at 1175 and 1086 cm^{-1} was assigned to the in-plane bending of the C—O—C group in PLGA. The absorption peaks at 2900 to 3000 cm^{-1} may have been due to the stretching vibrations of the C—H group. In addition, compared to the absorption bands of FA, the absorption bands at 1377 and 1753 cm^{-1} [Figure 2(b), PLGA/PVP/FA and PLGA/FA curves] were attributed to the introduction of FA, with peaks at both 1400 and 1755 cm^{-1}. The FTIR data qualitatively confirmed the loading of FA within PLGA/PVP. Some other FA signals, such as 937 and 1420 cm^{-1}, were difficult to observe in the PLGA/PVP/FA sample, likely because of the insensitivity of the FTIR technique or the fact that the vibration bands of FA overlapped with those of PLGA or PVP.

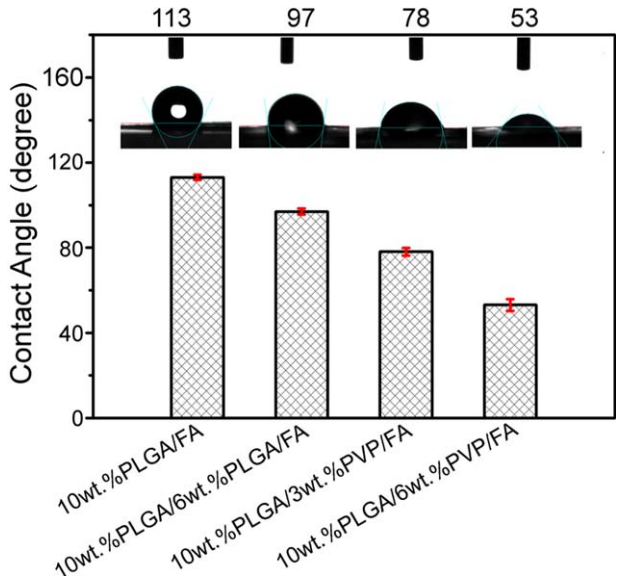

Figure 5. WCA results for membranes consisting of PLG/FA blend fibers, PLGA/PVP/FA coaxial fibers, and PLGA/PLGA/FA electrospun coaxial fibers. [Color figure can be viewed in the online issue, which is available at wileyonlinelibrary.com.]

Fabrication of Electrospun PLGA/PVP/FA Nanofibers

The formed PVP/FA solution with optimized FA loading percentage was then doped with PLGA nanofibers via coaxial electrospinning to form PLGA/PVP/FA composite nanofibers (Figure 1). For comparison, the pure PLGA/FA blend nanofibers, FA-doped PLGA/PLGA core–shell nanofibers, and FA-doped PLGA/PVP core–shell hollow nanofibers were also fabricated under similar electrospinning conditions. The presence of FA within the PLGA/PVP composite nanofibers was further confirmed by TEM (Figure 3).

The surface morphologies of the 10 wt % PLGA/FA blend, 10 wt % PLGA(shell)/6 wt % PLGA(core)/FA, 10 wt % PLGA(shell)/6 wt % PVP(core)/FA, and 10 wt % PLGA(shell)/3 wt % PVP(core)/FA nanofibers were observed via SEM (Figure 4). With the easy electrospinnability of PLGA, the incorporation of PVP, FA, or FA-loaded PVP did not seem to significantly alter the uniform and smooth fibrous morphology of the PLGA nanofibers. The diameters of the electrospun 10 wt % PLGA/FA blend nanofibers [Figure 4(a)], 10 wt % PLGA(shell)/6 wt % PLGA(-core)/FA [Figure 4(b)], 10 wt % PLGA(shell)/6 wt % PVP(core)/FA [Figure 4(c)], and 10 wt % PLGA(shell)/3 wt % PVP(core)/FA composite nanofibers [Figure 4(d)] were estimated to be 418 ± 40, 341 ± 21, 282 ± 16, and 324 ± 68 nm, respectively. The smaller diameters of the 10 wt % PLGA(shell)/6 wt % PLGA(-core)/FA, 10 wt % PLGA(shell)/6 wt % PVP(core)/FA, and 10 wt % PLGA(shell)/3 wt % PVP(core)/FA composite nanofibers compared to that of the pure PLGA nanofibers were presumably due to the increase of the solution conductivity or the solution viscosity, which was caused by the introduction of PVP or FA species into the electrospinning solution.

The data from the WCA measurements (Figure 5) implied a hydrophobic surface characteristic of the 10 wt % PLGA/FA blend nanofibers mats; this showed an average contact angle of 113°. The contact angles of the 10 wt % PLGA/6 wt % PLGA/FA, 10 wt % PLGA/3 wt % PVP/FA, and 10 wt % PLGA/6 wt % PVP/FA nanofibers mats were 97, 78, and 53°, respectively. PLGA is hydrophobic,[36,37] whereas PVP is hydrophilic,[38,39] and hence, the 10 wt % PLGA/FA blend nanofiber membrane and 10 wt % PLGA/10 wt % PLGA/FA nanofiber membrane possessed poor hydrophilicity and a relatively large contact angle. When PLGA and PVP were coaxially electrospun in an ideal case, the PLGA shell completely wrapped the PVP core. The hydrophilic nanofiber membrane WCA should have been the same as the hydrophilic PLGA electrospinning membrane. In practice, however, coaxial electrospinning could not be completely coaxial, and the PLGA shell PVP could not have a completely wrapped core either. The resulting fiber increased the hydrophilicity of the membrane, and the WCA became smaller.

Release of FA from PLGA/PVP/FA Composite Nanofibers

It has been reported that drug-release behaviors of drug-loaded nanofiber membranes are invariably controlled by the nanofiber morphology and, particularly, by drug–matrix interactions. The drug-loaded nanofiber membranes, which were fabricated by the electrospinning of a blended solution of drug and polymer, generally showed an initial burst release because of the high concentration of the drug distributed on the nanofiber surface. The release profiles of FA from the electrospun 10 wt % PLGA/FA blends nanofibers, 10 wt % PLGA/3 wt % PVP/FA composite nanofibers, 10 wt % PLGA/6 wt % PVP/FA composite nanofibers, and 10 wt % PLGA/6 wt % PLGA/FA composite nanofibers are shown in Figure 6. It was clear that both the 10 wt % PLGA/FA blend nanofibers and the 10 wt % PLGA/3 wt % PVP/FA composite nanofibers (0.5 wt % FA relative to PLGA) exhibited an obvious initial burst release. Within the first 6 h, approximate 55% of the drug was released, and most of the remaining drug (total release percentage > 80%) was released within the successive 190 h at a release speed of 0.15% per 10 h. In contrast, the FA released from the 10 wt % PLGA/6 wt % PVP composite nanofibers needed to go through two release phases, which were the initial fast release phase and a successive sustained slow release phase. About 40% of the FA

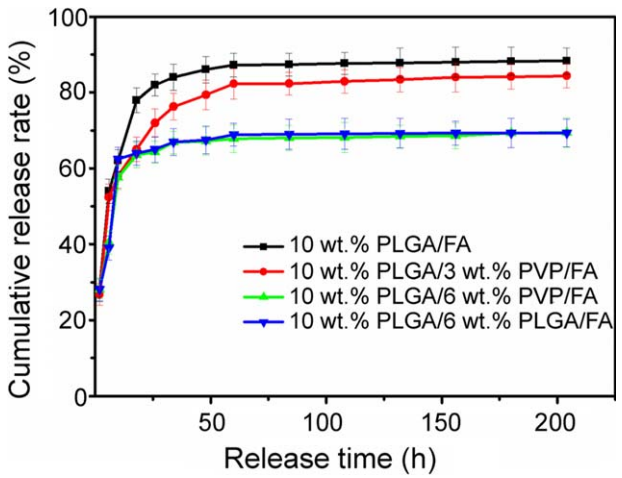

Figure 6. Contrast of release from the PLGA/FA blend fibers, PLGA/PVP/FA coaxial fibers, and PLGA/PLGA/FA coaxial fibers. [Color figure can be viewed in the online issue, which is available at wileyonlinelibrary.com.]

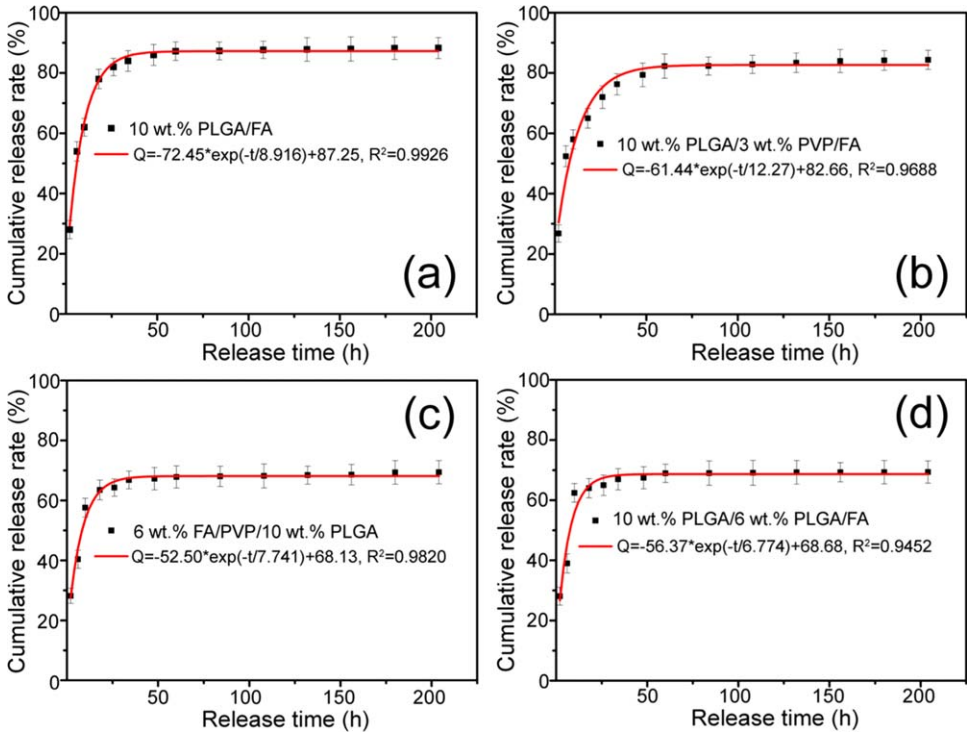

Figure 7. First-order kinetics equation fitting. [Color figure can be viewed in the online issue, which is available at wileyonlinelibrary.com.]

was released within the first 6 h, and around 70% FA was released by the 204th hour.

The fast release of FA from the PLGA/FA blend nanofibers was thought to be due to the fact that the physical interaction between FA and PLGA (e.g., hydrogen bonding) was not sufficiently strong. The same fast release of FA from the 10 wt % PLGA/3 wt % PVP/FA composite nanofibers was easily understandable because the direct physical integration of drugs within polymer nanofibers gave rise to a matrix-type drug-release featured with a fast release rate. This finding was in agreement with our previous work.[40] Therefore, for both PLGA/FA blend nanofibers and 10 wt % PLGA/3 wt % PVP/FA composite nanofibers, the weak force between the drug and the carriers unavoidably led to an initial burst release of the drug. However, for the 10 wt % PLGA/6 wt % PVP/FA composite nanofibers, the encapsulated FA drug was dissociated from the PVP to the solid PLGA matrix first and was then released from the solid PLGA matrix to the outer phase solution (Figure 1). With the combination of two different release profiles, the diffusion rate of the FA drug was significantly slowed, and thereby, the drug achieved a sustained release. The first-stage slight burst release of FA was attributed to the matrix-type release of FA predissociating from PVP during the electrospinning process.

The release of water-soluble drugs from a polymeric matrix is assumed to undergo several steps: water from the medium diffuses in through polymeric networks and dissolves the drug molecules. This is followed by diffusion out of the matrix and into the medium.[41] A Fickian kinetic expression derived for one-dimensional diffusion from monodispersed cylindrical matrices was used to analyze the FA release data of the PLGA-based composite nanofibers.

Drug-release kinetics from a polymeric nanofiber can be described with the first-order kinetic equation as follows:

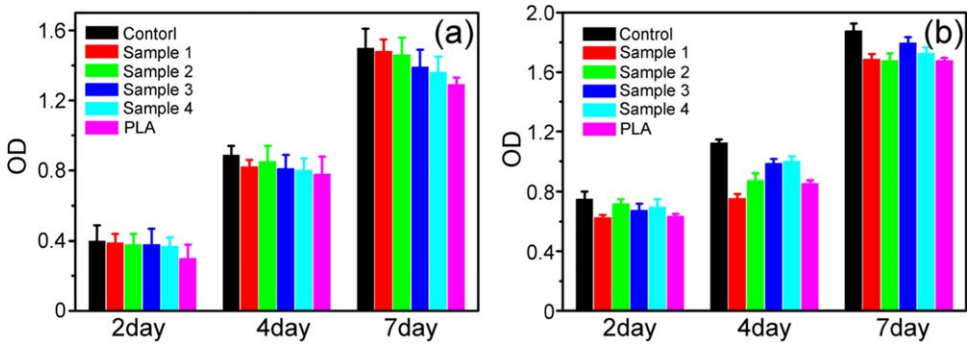

Figure 8. Test results for (a) NIH3T3 cytotoxicity and (b) ICE-6 cytotoxicity. [Color figure can be viewed in the online issue, which is available at wileyonlinelibrary.com.]

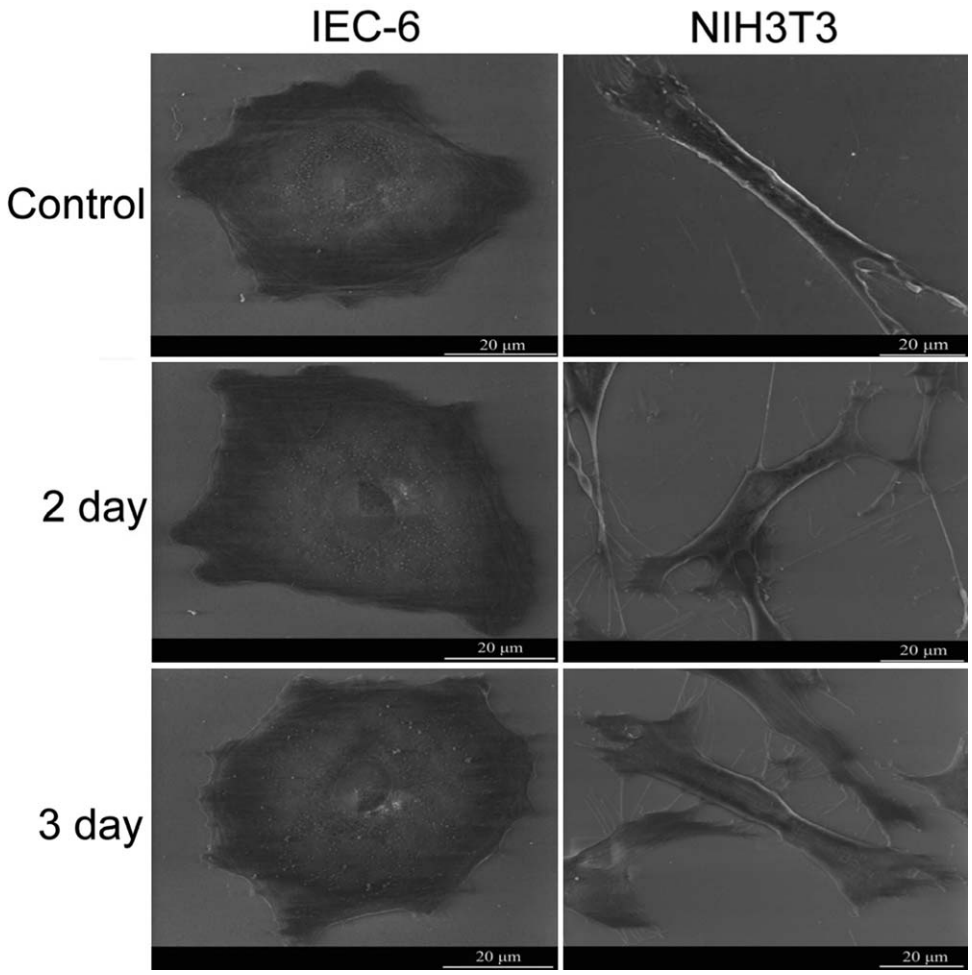

Figure 9. SEM photos of the IEC-6 cells and NIH3T3 cells before and after processing.

$$Q = \frac{M_t}{M_\infty} = Ae^{-\frac{t}{k}} + b$$

where Q is the cumulative release rate of FA, M_∞ is the mass of drug released as the time approaches infinity (or the total amount of drug encapsulated) and A, k, and b are three constants characteristic of the drug–polymer system. From the slope and intercept of the plot (Figure 7) of $\ln(M_t/M_\infty)$ versus $\ln t$ for the release of FA from the PLGA-based composite nanofibers, the goodness of fit (R^2) values were calculated to be 0.9926, 0.9688, 0.9820, and 0.9452, respectively. Hence, FA release in this case followed the Fickian diffusion mechanism; this indicated that drug diffusion was the primary factor in drug release.

Cytocompatibility Assay

In this study, the NIH3T3 and IEC-6 cell lines were cocultured with the prepared PLGA/PVP/FA composite nanofibrous membrane. After incubation for different periods, the PLGA/PVP/FA composite nanofibrous membrane was taken out, and CCK-8 detection was performed for the cells. By comparison with the control wells (without membrane in wells), the optical density (OD) value (OD and OD absorbed by the sample) of the test group and

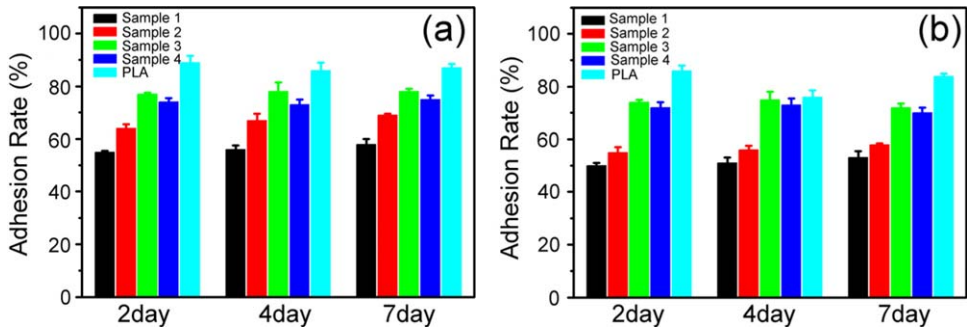

Figure 10. Adhesion rate of the (a) NIH3T3 cells and (b) IEC-6 cells to the PLGA/PVP/FA nanofiber membranes and PLA nanofiber membranes. [Color figure can be viewed in the online issue, which is available at wileyonlinelibrary.com.]

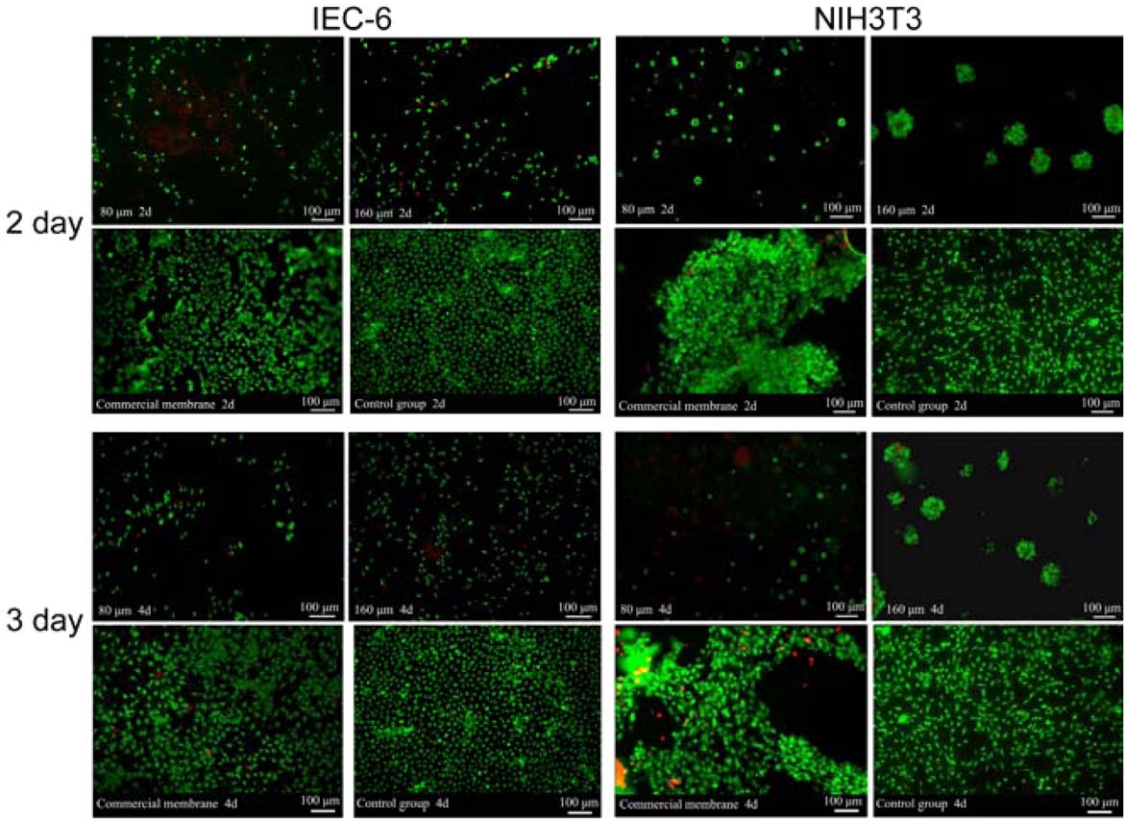

Figure 11. Fluorescence images of the IEC-6 cells and NIH3T3 cells incubated for 2 and 4 days with fluorescence staining. [Color figure can be viewed in the online issue, which is available at wileyonlinelibrary.com.]

the PLA nanofibrous membrane group had no significant variation. This showed that the composite nanofibrous membrane and commercial membrane had no cytotoxicity (Figure 8).

Images of the treated cells were obtained with a scanning electron microscope. Surface structure variations of the cells were observed directly to determine the effect of the treatments on the growth of the cells. Figure 9 shows that the cellular morphology of IEC-6 in the control group showed the presence of surface villus and a polygonal shape. This cellular morphology was also observed for the sample groups, which suggests that the cells were healthy. Compared to that of the control group, the micromorphology of cells treated with the degradation liquid of the PLGA/PVP/FA nanofibrous membrane had no obvious variation; this indicated that the degradation liquid of the material had no effect on the growth of the cells, and the PLGA/PVP/FA nanofibrous membrane was nontoxic (Figure 9).

Anti-Adhesion Activity

The NIH3T3 and IEC-6 cells were seeded on membranes with different thicknesses. After incubation for a period of time, an MTT test was performed for the cells adhered to the membranes. The light absorption value was in direct proportion to number of cells attached to the membranes and that were confluent across the membranes. The results show that the adherence rate of the two kinds of cells on the PLA nanofibrous membrane was the highest (90%). This adherence rate was significantly higher than on the 80 μm membranes (50%). For the other groups (samples 2, 3, and 4), the adherence rate was less than 80%. This indicated that compared to the commercial membranes, the PLGA/PVP/FA composite nanofibrous membrane showed good anticell adhesion performance (Figure 10).

In this study, we proposed a thickness of 120 μm as optimal as compared to thicknesses of 80, 160, and 200 μm. Images of the cell survival conditions were obtained only for the PLGA/PVP/FA composite nanofibrous membrane (thicknesses = 80 and 160 μm), PLA nanofibrous membrane, and normal adherence to the culture plates.

The images showed that when the NIH3T3 cells were cultured for 2 and 4 days, the adherence rates of the cells to the 80- and 160-μm nanofibrous membranes were low, and agglomeration was observed among cells. This may have been due to the fact that cells were not able to adhere to the nanofibrous membrane. However, for commercial nanofibrous membranes, the adherence rate of the cells was high, and an original cellular morphology was maintained. This indicated that their growth conditions on the membrane were favorable. This corroborated our previous results and suggested that the cells easily adhered to the commercial membrane. On the contrary, for the PLGA/PVP/FA composite nanofibrous membrane, the adherence rate of cells was low, and cells were hard to grow on the membrane. This indicated that the PLGA/PVP/FA composite nanofibrous membrane has good anticell adhesion performance. Fluorescence images are shown in Figure 10.

Similarly, fluorescence staining of the IEC-6 cells showed similar results, but compared to the NIH3T3 cells (agglomeration was observed among the cells), the IEC-6 cells were easier to spread on

all the membranes. This further validated the fact that the PLGA/PVP/FA composite nanofibrous membrane had good anticell adhesion performance; the fluorescence images are shown in Figure 11.

CONCLUSIONS

In summary, we developed a facile coaxial electrospinning approach to fabricate smooth and uniform PLGA/PVP/FA composite nanofibers with improved FA release profiles. The incorporation of drug-loaded PLGA/PVP nanofibrous membranes not only significantly improved the adhesion prevention activity of the nanofibers but also appreciably reduced the initial burst release of the drug. The combination of two pathways for FA dissociation, first from PVP to the PLGA fiber matrix and then from the PLGA fiber matrix to the release medium, was proven to be an efficient strategy to slow down the release rate of FA. This is important for biomedical applications requiring drugs to maintain long-term analgesic efficacy. With the proven cytocompatibility of the composite nanofibers, the concept for designing a PLGA/PVP nanofiber-based drug carrier may be extended to the preparation of other drug-delivery systems for various applications in tissue engineering and pharmaceutical science.

ACKNOWLEDGMENTS

The authors sincerely appreciate the support of Shanghai Major Construction Projects (contract grant number 11XK18BXKCZ1205), the Program of Shanghai Science and Technology Capacity Building Project Local Universities (contract grant number 11490501500), and Shanghai Graduate Innovation Entrepreneurial Training Projects.

REFERENCES

1. Hubbell, J. A.; Ashutosh, C. *Science* **2012**, *303*, 337.
2. Wang, X.; Ding, B.; Sun, G.; Wang, M.; Yu, J. *Prog. Mater. Sci.* **2013**, *58*, 1173.
3. Shao, S.; Zhou, S.; Li, L.; Li, J.; Luo, C.; Wang, J. *Biomaterials* **2011**, *32*, 2821.
4. Zheng, F.; Wang, S.; Wen, S.; Shen, M.; Zhu, M.; Shi, X. *Biomaterials* **2013**, *34*, 1402.
5. Nguyen, T.; Ghosh, C.; Hwang, S.; Chanunpanich, N.; Park, J. *Int. J. Pharm.* **2012**, *439*, 296.
6. Hu, X.; Liu, S.; Zhou, G.; Huang, Y.; Xie, Z.; Jing, X. *J. Controlled Release* **2014**, *185*, 12.
7. Yang, J.; Zha, L.; Yu, D.; Liu, J. *Colloids Surf. B* **2013**, *102*, 737.
8. Malherbe, I.; Sanderson, R.; Smit, E. *Polymer* **2010**, *51*, 5037.
9. Drexler, J.; Powell, H. *Acta Biomater.* **2011**, *7*, 1133.
10. Bayley, G.; Mallon, P. *Polymer* **2012**, *53*, 5523.
11. Ji, W.; Yang, F.; Seyednejad, H.; Chen, Z.; Hennink, W.; Anderson, J. *Biomaterials* **2012**, *33*, 6604.
12. Qi, R.; Guo, R.; Shen, M.; Cao, X.; Zhang, L.; Shi, X. *J. Mater. Chem.* **2010**, *20*, 10622.
13. Agarwal, S.; Greiner, A.; Wendorff, J. *Prog. Polym. Sci.* **2013**, *38*, 963.
14. Rogina, A. *Appl. Surf. Sci.* **2014**, *296*, 221.
15. Castillo-Ortega, M.; Montaño-Figueroa, A.; Rodríguez-Félix, D.; Munive, G.; Herrera-Franco, P. *Mater. Lett.* **2012**, *76*, 250.
16. Mariana, P.; Mirta, I.; Norma, E. *J. Appl. Polym. Sci.* **2008**, *107*, 1080.
17. Szentivanyi, A.; Chakradeo, T.; Zernetsch, H.; Glasmacher, B. *Adv. Drug Delivery Rev.* **2011**, *63*, 209.
18. Sun, B.; Long, Y.; Zhang, H.; Li, M.; Duvail, J. *Prog. Polym. Sci.* **2014**, *39*, 862.
19. Yu, H.; Jia, Y.; Yao, C.; Lu, Y. *Int. J. Pharm.* **2014**, *469*, 17.
20. Sai, M.; Zhong, S.; Tang, Y.; Ma, W.; Sun, Y.; Ding, D. *J. Appl. Polym. Sci.* **2014**, *131*, 40535.
21. Guo, B.; Glavas, L.; Albertsson, A. *Prog. Polym. Sci.* **2013**, *38*, 1263.
22. Zhang, J.; Wang, Q.; Wang, A. *Acta Biomater.* **2010**, *6*, 445.
23. Song, B.; Wu, C.; Chang, J. *Acta Biomater.* **2012**, *8*, 1901.
24. Lee, Y.; Lowe, J.; Gilby, E. *Int. J. Pharm.* **2010**, *383*, 244.
25. Puppi, D.; Piras, A.; Detta, N.; Dinucci, D.; Chiellini, F. *Acta Biomater.* **2010**, *6*, 1258.
26. Meng, Z.; Xu, X.; Zheng, W.; Zhou, H.; Li, L.; Zheng, Y. *Colloids Surf. B* **2011**, *84*, 97.
27. Nath, S.; Son, S.; Sadiasa, A.; Min, Y.; Lee, B. *Int. J. Pharm.* **2013**, *443*, 87.
28. Eun, J.; Won, S.; Yang, H. *J. Appl. Polym. Sci.* **2012**, *123*, 672.
29. Huang, W.; Shi, X.; Ren, L.; Du, C.; Wang, Y. *Biomaterials* **2010**, *31*, 4278.
30. Shen, H.; Hu, X.; Yang, F.; Bei, J.; Wang, S. *Biomaterials* **2009**, *30*, 3150.
31. Sophocleous, A.; Zhang, Y.; Schwendeman, S. *J. Controlled Release* **2009**, *137*, 179.
32. Vasite, R.; Mani, G.; Mauli Agrawal, C.; Katti, D. *Polymer* **2010**, *51*, 3706.
33. Chen, F.; Tang, Q.; Zhu, Y.; Wang, K.; Zhang, M.; Zhai, W.; Chang, J. *Acta Biomater.* **2010**, *6*, 3013.
34. Szentivanyi, A.; Chakradeo, T.; Zernetsch, H.; Glasmacher, B. *Adv. Drug Delivery Rev.* **2011**, *63*, 209.
35. Zhang, A.; Ding, D.; Ren, J.; Zhu, X.; Yao, Y. *J. Appl. Polym. Sci.* **2014**, *131*, 39890.
36. Nasouri, K.; Bahrambeygi, H.; Rabbi, A.; Mousavi Shoushtari, A.; Kaflou, A. *J. Appl. Polym. Sci.* **2012**, *126*, 127.
37. Fredenberg, F.; Wahlgren, M.; Reslow, M.; Axelsson, A. *Int. J. Pharm.* **2011**, *415*, 34.
38. Li, Q.; Yan, T.; Niu, S.; Zhao, Y.; Meng, X.; Zhao, Z. *Carbohydr. Res.* **2013**, *379*, 78.
39. Liu, S.; Zhao, J.; Ruan, H.; Wang, W.; Wu, T.; Cui, W. *Mater. Sci. Eng. C* **2013**, *33*, 1176.
40. Zhu, T.; Chen, S.; Lou, J.; Wang, J.; Li, Y.; Liao, J. *Chem. Ind. Eng. Prog.* **2014**, *33*, 463.
41. Fredenberg, S.; Wahlgren, M.; Reslow, M.; Axelsson, A. *Int. J. Pharm.* **2011**, *415*, 34.